JACS
JOURNAL OF THE AMERICAN CHEMICAL SOCIETY

Article

pubs.acs.org/JACS

Water-Containing Hydrogen-Bonding Network in the Active Center of Channelrhodopsin

Shota Ito,[†] Hideaki E. Kato,[‡] Reiya Taniguchi,[‡] Tatsuya Iwata,[†] Osamu Nureki,[‡] and Hideki Kandori*[,†]

[†]Department of Frontier Materials, Nagoya Institute of Technology, Showa-ku, Nagoya 466-8555, Japan

[‡]Department of Biophysics and Biochemistry, Graduate School of Science, The University of Tokyo, Bunkyo-ku, Tokyo 113-0032, Japan

Supporting Information

ABSTRACT: Channelrhodopsin (ChR) functions as a light-gated ion channel in *Chlamydomonas reinhardtii*. Passive transport of cations by ChR is fundamentally different from the active transport by light-driven ion pumps such as archaerhodopsin, bacteriorhodopsin, and halorhodopsin. These microbial rhodopsins are important tools for optogenetics, where ChR is used to activate neurons by light, while the ion pumps are used for neural silencing. Ion-transport functions by these rhodopsins strongly depend on the specific hydrogen-bonding networks containing water near the retinal chromophore. In this work, we measured protein-bound water molecules in a chimeric ChR protein of ChR1 (helices A to E) and ChR2 (helices F and G) of *Chlamydomonas reinhardtii* using low-temperature FTIR spectroscopy at 77 K. We found that the active center of ChR possesses more water molecules (9 water vibrations) than those of other microbial (2−6 water vibrations) and animal (6−8 water vibrations) rhodopsins. We conclude that the protonated retinal Schiff base interacts with the counterion (Glu162) directly, without the intervening water molecule found in proton-pumping microbial rhodopsins. The present FTIR results and the recent X-ray structure of ChR reveal a unique hydrogen-bonding network around the active center of this light-gated ion channel.

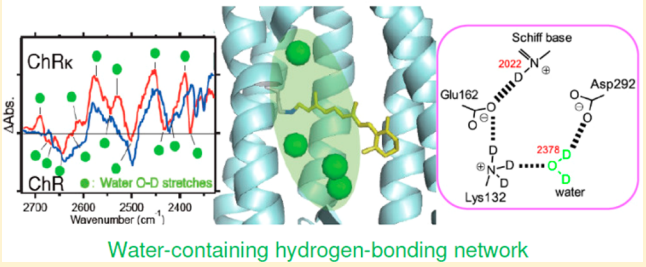

Water-containing hydrogen-bonding network

INTRODUCTION

Optogenetics has revolutionized neurosciences by using ion-transporting microbial rhodopsins as a tool for cell-specific control of neural activity.[1,2] Channelrhodopsin (ChR),[3,4] a light-gated cation channel, is used to activate neurons by light-triggered membrane depolarization, while light-driven ion pumps such as archaerhodopsin (AR), bacteriorhodopsin (BR), and halorhodopsin (HR) are used for neural silencing.[5−7]

Understanding ion-transport mechanism in these microbial rhodopsins[8] is particularly important for rational design of novel optogenetics tools. While ion-transport mechanisms have been extensively studied for BR and HR,[9,10] much less is known for the mechanism of cation conductance by ChR. Most importantly, why does ChR perform a passive transport of ions unlike other light-driven ion pumps? One of the reasons for the limited knowledge on ChR is difficulty in the sample preparation. Unlike for prokaryotic microbial rhodopsins, expression of ChR in *E. coli* has been difficult. Even though channelrhodopsins can be expressed in other cells, purified ChR1 and ChR2 are less stable than their bacterial homologues. Consequently, structural information on ChR has been scarce. However, Kato et al. recently determined the structure of a chimeric protein of ChR1 (helices A to E) and ChR2 (helices F and G) of *Chlamydomonas reinhardtii* (C1C2).[11] This opened the way for understanding of molecular mechanism of the ChR function in atomic details.

One of the key elements in understanding the structure−function relationship of ChR is to reveal its hydrogen-bonding network in the active center. Of a particular importance are protein-bound water molecules, which do not simply occupy protein cavities, but participate in the light-induced structural changes and assist ion-transport.[12,13] The X-ray structure of C1C2 shows 10 internal water molecules.[11] In addition, the channel cavity at the extracellular side may contain more bound water molecules, which are not seen in the crystal structure due to their mobility, but are suggested by MD simulations.[14] Low-temperature FTIR spectroscopy is a powerful method to study hydrogen-bonding networks including water molecules, in particular those around retinal Schiff base of rhodopsins.[15,16] In fact, from the comprehensive studies of water vibrations of various rhodopsins, we found that a strongly hydrogen-bonded water molecule (O−D stretch at <2400 cm^{-1}) that bridges the Schiff base and its counterion is necessary for proton-pumping activity.[16,17] This suggests that a strongly hydrogen-bonded water molecule is the functional determinant of light-driven proton pumping. Then, how are the hydrogen-bonding network and protein-bound water molecules organized in ChR? Even though ChR is a microbial rhodopsin, its channel

Received: October 23, 2013
Revised: January 25, 2013
Published: February 10, 2014

dx.doi.org/10.1021/ja410836g | *J. Am. Chem. Soc.* 2014, 136, 3475−3482

function is unique, which suggests a distinctive hydrogen-bonding pattern. However, it has been proposed that ChR has some proton-pumping activity.[18,19] In this study, we applied low-temperature FTIR spectroscopy to C1C2 chimeric ChR at 77 K, where the primary photointermediate is formed by the all-trans to 13-cis photoisomerization. It should be noted that at 77 K, light-induced structural changes are limited to the immediate vicinity of the retinal chromophore, so that the hydrogen-bonding network in the unphotolyzed state and its changes upon retinal photoisomerization can be analyzed in detail by difference FTIR spectroscopy.

RESULTS AND DISCUSSION

ChR_K Minus ChR Infrared Spectra in the 1800−850 cm^{-1} Region. The C1C2 chimera of ChR was prepared as described previously (see Experimental Section).[11] The 0.2 mg of purified protein in 0.05% *n*-dodecyl-*β*-D-maltoside (DDM) was reconstituted into lipid bilayers of phosphatidyl glycerol (PG). Figure 1 shows the light-induced difference FTIR spectra

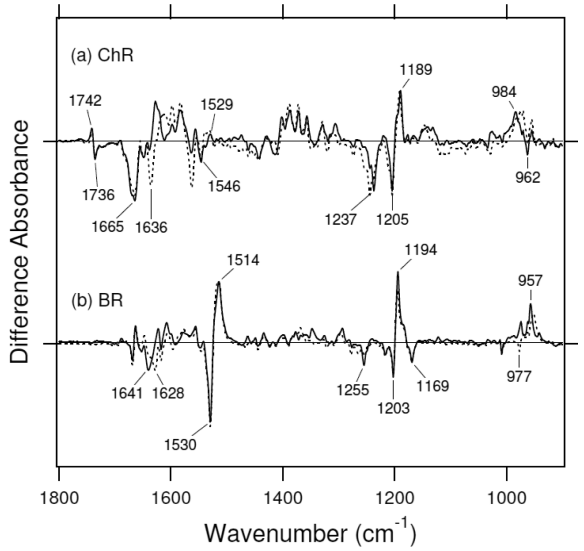

Figure 1. The ChR_K minus ChR (a) and the BR_K minus BR (b) spectra in the 1800−850 cm^{-1} region measured at pH 7 and 77 K upon hydration with H_2O (solid line) and D_2O (dotted line). One division of the *y*-axis corresponds to 0.0025 absorbance units. The spectra in (a) are shown without changing the amplitude, while those in (b) are multiplied by 0.09. The data in (b) are reproduced from ref 55.

of ChR in the 1800−850 cm^{-1} region, which were measured at 77 K after the hydration with H_2O (solid lines) and D_2O (dotted lines) (absolute absorption spectra and difference spectra in the 4000−800 cm^{-1} region are shown in Supporting Information, SI, Figures S1 and S2, respectively). The shape of the difference spectra between ChR_K and ChR for the C1C2 chimera is similar to that reported previously for ChR2.[20−22] A pair of peaks at 1546 (−)/1529 (+) cm^{-1} corresponds to the ethylenic stretching vibration of ChR and the red-shifted K (P1 or P500) state, respectively. In the C−C stretching vibrations region of the retinal, a negative band at 1205 cm^{-1} is assignable to the C14−C15 stretching vibration of all-*trans* retinal, and a positive band at 1189 cm^{-1} is assigned to the C10−C11 and C14−C15 stretching vibrations of the 13-*cis* retinal after the formation of the K state. The most intense hydrogen-out-of-plane (HOOP) band was observed at 984 cm^{-1} (in H_2O) and 975 cm^{-1} (in D_2O). The C=N stretching vibrations of the protonated Schiff base in ChR were observed at 1665 cm^{-1} (C=NH) and 1636 cm^{-1} (C=ND), which reproduces the results obtained by resonance Raman spectroscopy for ChR2.[23] The frequency upshift of the C=N stretching vibration in H_2O is caused by its coupling to the N−H bending vibration of the Schiff base, and the difference in frequency between H_2O and D_2O has been regarded as a measure of hydrogen-bonding strength of the Schiff base.[24] Such difference for ChR (29 cm^{-1}) is much larger than that of BR (13 cm^{-1}), suggesting that the hydrogen bond of the Schiff base in ChR is stronger than in BR. The hydrogen bonding strength of the Schiff base will be discussed in more detail below, based on the data from its N−D stretching region. Large structural changes of the peptide backbone are reflected in the negative amide-I band at 1665 cm^{-1}, which overlaps with the Schiff base vibrations, but does not shift in D_2O. The large secondary structural perturbation at 77 K, consistent with the previous reports,[20,23] is unique for ChR, in clear contrast to other microbial rhodopsins.

In the ChR_K minus ChR difference spectra (Figure 2), intense bands were observed at 1742 (+)/ 1736 (−) cm^{-1}.

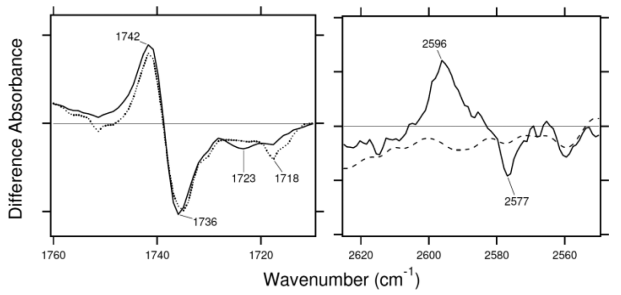

Figure 2. Left panel: Enlarged spectra from Figure 1a in the 1760−1710 cm^{-1} region. Solid and dotted lines represent the spectra in H_2O and D_2O, respectively. One division of the *y*-axis corresponds to 0.0002 absorbance units. Right panel: The ChR_K minus ChR spectra in the S−H stretching frequency region (solid line) in H_2O. Dashed line represents the difference of two spectra without illumination. One division of the *y*-axis corresponds to 0.00002 absorbance units.

Nack et al. reported similar bands at 1742 (+)/ 1735 (−) cm^{-1} for ChR2, and assigned them to Asp156.[22] Since both ChR1 and ChR2 possess aspartate at the homologous position, the similar bands most likely originate from Asp195 (Asp156 in ChR2) in the chimera. Interestingly, the bands at 1742 (+)/ 1736 (−) cm^{-1} do not exhibit downshift in D2O (Figure 2). This observation is in a stark contrast to a negative peak at 1723 cm^{-1}, which is shifted to 1718 cm^{-1} in D_2O. The negative peak at 1723 cm^{-1} possibly originates from Glu129 (Glu90 in ChR2), as can be inferred from the similarity to the reported frequency.[25] It should be noted that the spectral shape in the protonated carboxylic acids region (Figure 2 Left) can be fully accounted for by the changes of Asp195 and Glu129 vibrations. This suggests that two carboxylates near the Schiff base, Glu162 and Asp292, are deprotonated under the present experimental conditions.

On the basis of their FTIR results, Nack et al. proposed a crucial hydrogen bonding interaction between Cys128 and Asp156 in ChR2.[22] In contrast, according to the X-ray structure, there is no direct interaction between Cys167 (Cys128 in ChR2) and Asp195 in the C1C2 chimera, and Cys167 points toward the retinal chromophore rather than Asp195 (see below).[11] We observed S−H stretching bands at

dx.doi.org/10.1021/ja410836g | J. Am. Chem. Soc. 2014, 136, 3475−3482

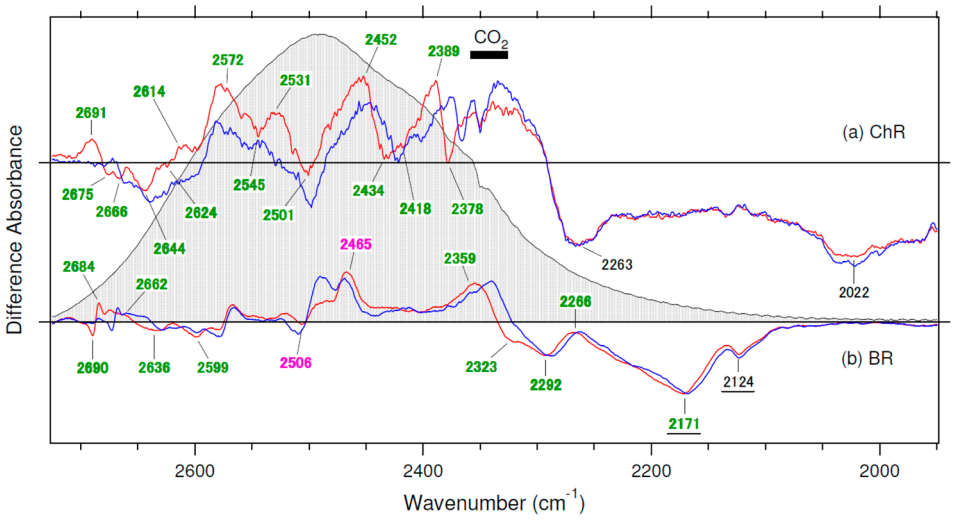

Figure 3. The ChR_K minus ChR (a) and the BR_K minus BR (b) spectra in the 2725−1930 cm^{-1} region measured at pH 7 and 77 K upon hydration with D_2O (red) or $D_2{}^{18}O$ (blue). Green-labeled frequencies correspond to those identified as O−D stretching vibrations of water. Purple-labeled and underlined frequencies in panel b are O−D stretches of Thr89 and N−D stretches of the Schiff base in BR, respectively. Light gray spectrum shows the water O−D stretching vibrations region. One division of the *y* axis corresponds to 0.0002 absorbance units. The data in (b) are reproduced from ref 56.

2596 (+)/2577 (−) cm^{-1} (Figure 2). According to the X-ray structure, Cys167 is located near the chromophore (3.3 Å between the cysteine sulfur and C13 atom of retinal), and other Cys are located far from the retinal chromophore (>9 Å). It is thus likely that the signal we observed originates from Cys167. The stretching frequency of cysteine S−H is in the 2580−2525 cm^{-1} region,[26,27] and the high frequency at 2590−2580 cm^{-1} indicates that Cys167 does not form a hydrogen bond in the C1C2 chimera, consistent with the X-ray structure.[11]

Comparison of the X−D Stretching Vibrations of ChR and BR. X−D stretching vibrations of protein and water molecules appear in the 2725−1930 cm^{-1} region in D_2O (Figure 3). A spectral comparison of the samples hydrated with D_2O and $D_2{}^{18}O$ identifies O−D stretching vibrations of water molecules, changing their frequencies upon retinal photoisomerization. The signal amplitudes in ChR (on the order of 10^{-5} absorbance units) are smaller than those of other microbial rhodopsins, but we were able to examine and reproduce three times the isotope shift of water in the whole O−D stretching region (Figure 3). We assigned green-tagged bands in Figure 3a to the O−D stretching vibrations of water. Since the red and blue spectra have baseline drift differences, the detailed analysis with the baseline correction is shown in SI Figure S3. We identified 9 negative bands as the water O−D stretching vibrations of ChR at 2675, 2666, 2644, 2624, 2545, 2501, 2434, 2418, and 2378 cm^{-1}, and 6 positive bands as the water O−D stretching vibrations of ChR_K at 2691, 2614, 2572, 2531, 2452, and 2389 cm^{-1}. The unbalanced numbers of positive and negative bands suggest that positive peaks contain vibrations of multiple water molecules. It should be noted that the isotope shifts of water are observed in the whole water O−D stretching region (the gray curve in Figure 3), from 2700 to 2350 cm^{-1}, which is not common for rhodopsins, as discussed below. In contrast, no water bands at low frequencies typical for proton pumps are observed at <2350 cm^{-1}.

Identification of protein-bound waters in ChR provides an important structural information related to function. First, the water band of ChR at 2378 cm^{-1} is noteworthy. BR exhibits unusually low frequency water vibrations at 2323, 2292, and 2171 cm^{-1} (Figure 3b), which are identified as the 3 water molecules involved in the pentagonal cluster in the Schiff base region.[28] From the comprehensive studies of water vibrations of various rhodopsins, we found that strongly hydrogen-bonded water molecules (O−D stretch at <2400 cm^{-1}) are always present in rhodopsins exhibiting proton-pumping activity.[16,17] For example, green-absorbing proteorhodopsin (PR) from marine bacteria,[29] *Gloeobacter* rhodopsin (GR) from cyanobacteria,[30] and a fungal *Leptosphaeria* rhodopsin (LR)[31] exhibit water O−D stretching vibrations at 2315, 2295, and 2257 cm^{-1}, respectively. This strong correlation between water hydrogen bond and proton-pumping function allowed us to conclude that a strongly hydrogen-bonded water molecule is the functional determinant of proton pumping. Even though ChR has no water bands at <2350 cm^{-1}, the water band at 2378 cm^{-1} (Figure 3) falls into the category of strongly hydrogen-bonded waters. Therefore, from the empirical correlation discussed above, one could suggest that ChR could be a light-driven proton pump. Interestingly, electrophysiological measurements by Feldbauer et al. suggested that ChR has a weak proton pumping activity.[18]

Second, the number of water bands in ChR is intriguing. We have studied hydrogen-bonding alteration of water for many microbial and animal rhodopsins under the same conditions (upon retinal isomerization at 77 K). In the unphotolyzed states of proton pumps, we observed 6 water bands for BR,[28] 6 water bands for GR,[30] 5 water bands for *Natronomonas pharaonis* sensory rhodopsin II (it is a sensor, but pumps protons in the absence of the transducer),[32] 4 water bands for PR,[29] and 4 water bands for LR.[31] In the unphotolyzed states of other microbial rhodopsins, we observed 4 water bands for *Natronomonas pharaonis* halorhodopsin,[33] 3 water bands for *Anabaena* sensory rhodopsin (ASR),[34] and 2 water bands for *Neurospora* rhodopsin.[35] In the unphotolyzed states of animal rhodopsins, we observed 6 water bands for bovine rhodopsin,[36] 8 water bands for squid rhodopsin,[37] 7 water bands for monkey green opsin, and 6 water bands for monkey red opsin.[38] Thus, microbial and animal rhodopsins show changes in 2−6 and 6−8 water bands upon retinal photoisomerization at 77 K,

dx.doi.org/10.1021/ja410836g | J. Am. Chem. Soc. 2014, 136, 3475−3482

respectively (SI Table S1). Smaller numbers of altered water molecules in microbial rhodopsins compared to animal rhodopsins may originate from the specific differences in each protein's environment, or from the structural changes upon all-trans to 13-cis isomerization in microbial rhodopsins being smaller than those upon 11-cis to all-trans isomerization in animal rhodopsins.[16] It should be noted that even though ChR is a microbial rhodopsin, 9 water bands were observed in this study. This is unusual, as the number is even larger than for animal rhodopsins. The present experimental observation is consistent with the recent theoretical calculations results,[14] and extra water molecules possibly reside in the channel cavity.

Finally, the spectral distribution of water bands in ChR is also unique. The water O−D stretches of BR are clustered in the weak hydrogen bond region (at 2700−2600 cm^{-1}), and in the very strong hydrogen bond region (at 2350−2150 cm^{-1}).[28] Such a large separation of water bands originates from weak vibrational coupling of the stretches in each water, being presumably due to strong association of the waters to negative charges of Asp85 and Asp212 in the Schiff base region of BR. In contrast, 9 water O−D stretches in ChR distribute much more evenly, being present in the weak hydrogen bond region (2700−2600 cm^{-1}), moderate hydrogen bond region (2600−2450 cm^{-1}), and strong hydrogen bond region (2450−2350 cm^{-1}), but absent in the very strong hydrogen bond region (2350−2150 cm^{-1}). The unique distribution of water molecules vibrations in ChR must be coupled to its specific protein−water interactions. In fact, ChR possesses a polar cavity penetrating from the extracellular side into the region neighboring the retinal chromophore.[11] Even though some of the water molecules are invisible in the crystal structure, recent MD simulation suggests the presence of a number of extra water molecules in this cavity (Kato et al. submitted), consistent with the results by Watanabe et al.[14] In this regard, formation of the ice-like structure of water in ChR is particularly revealing. Water stretching vibrations exhibit dramatic transition upon freezing, from 2600−2450 cm^{-1} to 2450−2200 cm^{-1}. Although many of the previous FTIR studies were performed at 77 K, observation of water vibrations at 2450−2300 cm^{-1} is very rare in rhodopsins,[28−38] suggesting that most protein-bound water molecules are isolated and ice-like structure is not formed. In contrast, observation of 3 negative bands at 2450−2300 cm^{-1} in ChR may suggest the formation of an ice-like structure in the channel cavity.

The frequency region shown in Figure 3 also contains X−D stretching vibrations other than those of water molecules. N−D stretching vibration of the protonated Schiff base may be assigned to either 2263 or 2022 cm^{-1} band. The corresponding band for BR appears at 2200−2100 cm^{-1}.[39] Since ChR has stronger Schiff base hydrogen bond than BR, as shown in Figure 1, the 2022 cm^{-1} band is a better candidate for the Schiff base N−D stretch. The corresponding positive band is located at >2300 cm^{-1}, indicating that retinal isomerization weakens the hydrogen bond of the Schiff base, similar to other microbial rhodopsins.[15] Then, the origin of the negative 2263 cm^{-1} band is intriguing. In the case of BR, retinal isomerization perturbs Arg82, a member of the complex Schiff base counterion, producing similar spectral signatures, but of a smaller amplitude.[39] Since the homologous Arg is not involved in the Schiff base counterion in ChR, according to the X-ray structure, other group(s) may contribute to the signal. In the BR_K minus BR spectrum, the bands at 2506 (−)/2465 (+) cm^{-1} were assigned to the O−D stretching vibrations of Thr89 (tagged in purple in Figure 3b).[40] Since the corresponding Thr is conserved in ChR, it is possible that the bands at 2501 (−)/2452 (+) cm^{-1} may have a similar origin. It is likely because the isotope shift of water is smaller for the bands at 2501 (−) and 2452 (+) cm^{-1}, suggesting the involvement of other vibrations.

UV−Visible Analysis of ChR Mutants. While the assignment of vibrational bands is simplified by isotope labeling, we use site-directed mutagenesis for positional identification of amino acids and protein-bound water molecules, as was done for BR.[28] In the present work, we focused on the three amino acids in the Schiff base region, Lys132 (Lys93 in ChR2), Glu162 (Glu123), and Asp292 (Asp253). Glu162 and Asp292 correspond to the counterion-forming negatively charged Asp85 and Asp212 in BR, respectively. According to the X-ray structure of BR, the distances from the Schiff base nitrogen are 3.7, 4.3, and 2.7 Å to the nearest oxygen of Asp85, Asp212, and a nearest water molecule, respectively.[41] It is known that Asp85 is the principal counterion and Asp212 is the secondary counterion in BR, and the spectral red-shift is much larger in D85N than in D212N.[42] In BR, a water molecule bridges the Schiff base and Asp85, and the strong interaction in the [SB−water−D85] complex is functionally important, ensuring the primary proton transfer, where the water molecule is a determinant of proton pumping ability.[16,17]

But how does the Schiff base region in ChR compare to this arrangement? The FTIR spectroscopy presented above suggested a deprotonated state of Glu162 and Asp292, similar to BR, from the analysis of the 1760−1710 cm^{-1} region (Figure 2, Left). According to the X-ray structure of ChR, the distances from the Schiff base nitrogen to the nearest oxygen are 3.4, 3.0, and 4.4 Å for Glu162, Asp292, and a nearest water molecule, respectively.[11] Two points should be stressed in comparison with BR. First, the distance between the Schiff base and the closest water (4.4 Å) is too long to form a hydrogen bond, suggesting that water is not the hydrogen-bonding acceptor of the Schiff base in ChR. Second, the distance to Asp292 is closer than that to Glu162, suggesting that Asp292 may be the principal counterion in the ground state. However, when we purified ChR WT, E162Q, K132A, and D292N, we found that the UV−vis absorption spectra of E162Q, K132A, and D292N show red-shift by 11, 7, and 4 nm, respectively (Figure 4). This result strongly suggests that both Glu162 and Asp292 possess negative charges (deprotonated), and that Glu162 is the principal counterion like in BR. We note that similar results were reported for ChR2.[43] Apparent contradiction between the crystal structure and the UV−vis spectroscopy results could be interpreted by the orientation of the Schiff base hydrogen bond. Namely, in the crystal structure, the Schiff base N−H bond may points toward Glu162 and the distance between the proton of the Schiff base and the carboxyl oxygen of Glu162 would be shorter than that for Asp292. Another possibility is a different pH of the crystallization solution. Although the present spectroscopic study was performed at pH 7−8, the chimeric ChR was crystallized at pH 5.8. Thus, in the crystal, Glu162 might be protonated, and the hydrogen-bond network in the active center would be different from the physiological one. It should also be noted that the spectral red-shift upon the counterion neutralization is smaller in ChR than in BR, possibly originating from different hydrogen-bonding network in the Schiff base region of ChR.

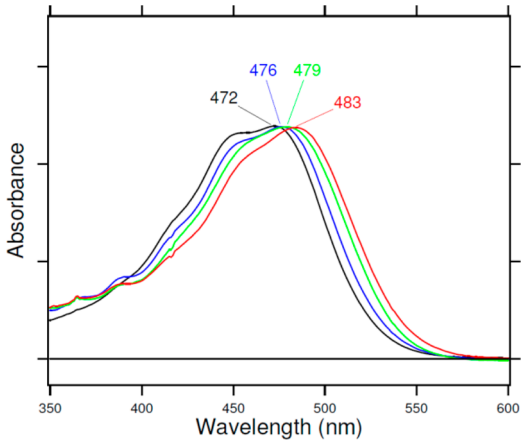

Figure 4. The absorption spectrum of ChR WT (black), D292N (blue), E162Q (red), and K132A (green). The samples are solubilized in 150 mM NaCl, 50 mM Tris-HCl, pH 8.0, 5% glycerol, 0.05% DDM, and 0.01% CHS.

FTIR Analysis of ChR Mutants. To further study the hydrogen-bonding network in ChR, we compared difference FTIR spectra of WT and the mutant proteins (K132A, E162Q, and D292N). SI Figure S4 shows similarity of all spectra in the 1800−850 cm^{-1} region, except for the amide-I region. This indicates normal photoisomerization processes in all mutants, but suggests that protein structural changes differ. The absence of changes in amide-I vibrations for all mutants implies that the hydrogen-bonding network in the Schiff base region is tightly coupled to the secondary structure alteration in ChR. Figure 5 shows the frequency region of X−D stretching vibrations under weak (2725−2580 cm^{-1}) and strong (2400−1950 cm^{-1}) hydrogen bonding conditions. Because of low expression level of the mutants, the S/N ratio in the 2580−2400 cm^{-1} region was not sufficient for the analysis and is not shown.

Figure 5 clearly shows that the negative band at 2022 cm^{-1} is preserved in D292N, but disappears in E162Q and K132A. This observation is consistent with the UV−vis spectra, and strongly supports its origin from the N−D stretch of the Schiff base. The lack of effect of charge neutralization at the position 292 can be interpreted by the absence of direct hydrogen bonding interaction between the Schiff base and Asp292. The observed 4 nm red-shift in the visible absorption is probably caused by electrostatic effect. In contrast, charge neutralization at the position 162 upshifts the N−D stretch of the Schiff base by 150−130 cm^{-1}. Therefore, we propose that Glu162 is the hydrogen-bonding acceptor of the Schiff base (Figure 6). Similar upshift for K132A further suggests the presence of complex hydrogen-bonding network involving Lys132.

The opposite mutation effect was observed for water O−D stretching vibrations in the strong hydrogen bond region (2389 (+) /2378 (−) cm^{-1}). Namely, the bands are preserved in E162Q, but disappear in D292N. These results suggest that the strongly hydrogen-bonded water molecule (with the spectral signature at 2389 (+) /2378 (−) cm^{-1}) is located in the Schiff base region, but is not directly bound to E162. While the bands also disappear in K132A, it is likely that new water bands appear at 2331 (+), 2281 (−), and 2237 (+) cm^{-1}. The reduced side chain volume resulting from the K132A mutation may allow for entrance of multiple water molecules, forming a new strongly hydrogen-bonded network. We propose that a strongly hydrogen-bonded water molecule (seen at 2389 (+) /2378 (−) cm^{-1}) interacts with Lys132 and Asp292, possibly bridging the ion-pair (Figure 6). According to the X-ray structure, one water molecule is present near Asp292 and Lys132 (Figure 6).[11]

Left panel of Figure 5 shows that weakly hydrogen-bonded water bands (in the 2700−2600 cm^{-1} region) are not strongly affected by these mutations, although the 2624 cm^{-1} band seems to have disappeared. This suggests that these weakly hydrogen bonded water molecules are not located in the Schiff base region, but may reside in the channel cavity (blue region in the upper panel of Figure 6). Unfortunately, the mutation effect on the ice-like water structure with the spectral signature at 2450−2400 cm^{-1} (Figure 3) was not accurately measured because of the insufficient S/N ratio for mutants. It should be noted that the channel cavity is spatially restricted, and bound water molecules may not be as free as in aqueous solution. Molecular properties of such bound water molecules in the channel cavity are intriguing, and their structural analysis is our future focus.

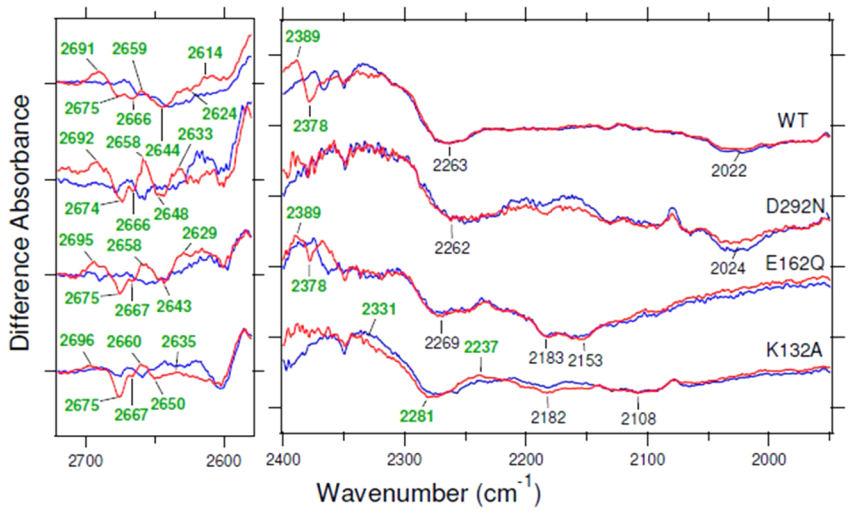

Figure 5. The ChR_K minus ChR spectra in the 2725−2580 cm^{-1} region (left panel) and 2400−1950 cm^{-1} region (right panel) measured at pH 7 and 77 K upon hydration with D_2O (red) or $D_2{}^{18}O$ (blue) in WT, D292N, E162Q, and K132A. Green-labeled frequencies correspond to those identified as O−D stretching vibrations of water. One division of the *y* axis corresponds to 0.00015 absorbance units.

dx.doi.org/10.1021/ja410836g | *J. Am. Chem. Soc.* 2014, 136, 3475−3482

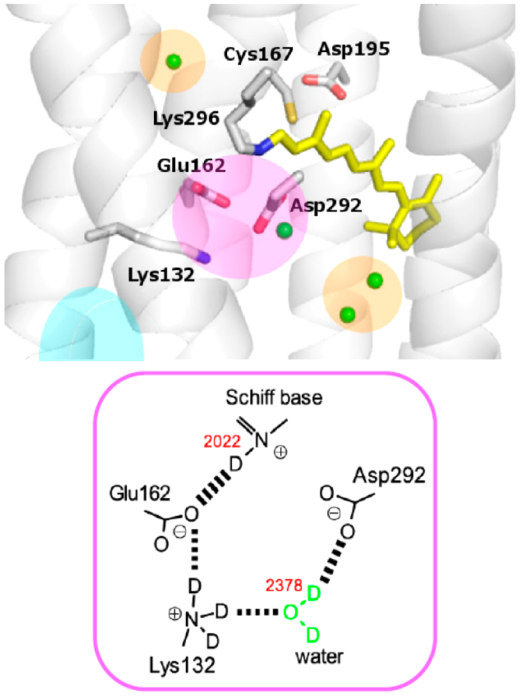

Figure 6. Upper panel: X-ray crystallographic structure of ChR (PDB entry 3UG9). The membrane normal is approximately in the vertical direction, and upper and lower regions correspond to the cytoplasmic (CP) and extracellular (EC) sides, respectively. The retinal chromophore, which is bound to Lys296 (Lys257 in ChR2), is shown by yellow stick model. Protein-bound water molecules within 5 Å from the retinal chromophore are shown by green spheres. Bottom panel: Schematic drawing of the hydrogen-bonding network in the Schiff base region of ChR. The red numbers are the N−D and O−D stretching frequency of the Schiff-base and water, respectively, in cm^{-1} obtained in the present work. Thicker lines denote stronger hydrogen bonds.

Unique Hydrogen-Bonding Network in the Active Center of Channelrhodopsin. On the basis of the present FTIR study and the recent X-ray structure, we propose a model of the hydrogen-bonding network in the Schiff base region of ChR shown in Figure 6. The lack of Glu162 and Asp292 signals in the protonated carboxylic acids region (Figure 2, Left) suggests deprotonated state of these groups. Frequencies of COO^- stretching vibrations of Glu162 and Asp292 are possibly located at 1413 (−)/1402 (+) cm^{-1} and 1442 (−)/1387 (+) cm^{-1}, respectively, because these bands disappear in E162Q and D292N mutants (SI Figure S4).

Strong hydrogen bond of the Schiff base in ChR was originally reported in the resonance Raman study,[23] where frequency difference of the C=N stretch in H_2O and D_2O was correlated to the hydrogen-bonding strength. It was confirmed in the present study (Figure 1), which is further supported by the N−D stretch being at a very low frequency (2022 cm^{-1}; Figure 3). The N−D stretch frequency (2022 cm^{-1}) is lower than those of other microbial rhodopsins (SI Table S2), and the only comparable frequency was seen for bovine rhodopsin (2012, 1966 cm^{-1}).[36] Interestingly, bovine rhodopsin has no bridging water molecule between the Schiff base and its counterion.[44] All of this implies that the Schiff base in ChR forms a direct hydrogen bond with its counterion, Glu162, without an intervening water molecule. Our model in Figure 6 is based on the observation for the chimeric C1C2 protein, but the direct hydrogen-bonding interaction is presumably true for ChR2 as well, judging from the resonance Raman data.[23]

In other microbial rhodopsins, a water molecule commonly serves as the hydrogen-bonding acceptor of the Schiff base. Such Schiff base water is observed in the X-ray structures of ASR,[45] xanthorhodopsin (XR),[46] and *Exiguobacterium sibiricum* Rhodopsin (ESR),[47] with the distances from the Schiff base nitrogen being 2.6, 2.9, and 2.8 Å, respectively. The function of this water is to serve not only as the hydrogen-bonding acceptor for the Schiff base, but also as the hydrogen-bonding donor for the counterion, where strong hydrogen-bonding of water is a prerequisite for the proton pumping function.[16,17] In the case of ChR, the water molecule is farther away from the Schiff base (4.4 Å) and, consequently, the water does not bridge the ion pair, the Schiff base and Glu162. However, this water molecule is likely to be involved in a different hydrogen-bonding network, interacting with Asp292 and Lys132 (Figure 6).

While the model in Figure 6 is consistent with the present FTIR results and the X-ray structure, it may contradict the present UV−vis results. Neutralization of Glu162 and Asp292 yields the spectral red-shift by 11 and 4 nm, respectively, while in the case of BR, D85N, and D212N mutants exhibit spectral red-shift by about 40 and 15 nm. From much smaller red-shifts in ChR, one might suspect that these carboxylates are protonated. Recent theoretical calculations suggested that Glu162 is protonated in the C1C2 chimera, while the corresponding residue (Glu123) in ChR2 is deprotonated.[14] It should however be noted that neutralization of the Schiff base counterion in XR and GR, other microbial rhodopsins, causes smaller spectral red-shift (a few nm) than in ChR,[48,49] and the present vibrational analysis supports deprotonated state of Glu162 and Asp292. Color tuning mechanism involves many complex factors, and vibrational analysis provides more local structural information. The hydrogen-bonding strength of the Schiff base is unchanged for D292N mutant, but its stretching frequency is up-shifted by 150−130 cm^{-1} for E162Q (Figure 5), which provides additional experimental support for our model. Further experimental and theoretical efforts are needed to understand the detailed hydrogen-bonding structure of the Schiff base region and color tuning mechanism of ChR.

The unique hydrogen-bonding network in the Schiff base region of ChR is possibly correlated to the specific conformational changes needed for the channel function. Unusually large changes in amide-I vibrations amplitude at very low temperatures (77 K) are characteristic for ChR2.[20,23] Time-resolved IR spectroscopy showed that the amide-I changes occur in 500 fs, and this surprisingly fast protein response indicates a tight coupling of retinal photoisomerization and protein structural changes.[50] The present study reveals that the large changes in amide-I vibration are absent for the mutants of the Schiff base region (K132A, E162Q, D292N) (SI Figure S4). This observation suggests an important role of hydrogen-bonding network in the Schiff base region for the structural perturbation of the protein.

Finally, the DC gate (Asp195 and Cys167 in the C1C2 chimera, Figure 6) structure should be discussed. It is well-known that the DC gate mutation (D156A/C128S of ChR2) significantly slows down the photocycle, so that the opening and closing can be easily controlled by blue and yellow light, respectively.[51] On the basis of their FTIR results, Nack et al. proposed a model of the DC gate, in which the S−H group of Cys donates a hydrogen-bond to the C=O group of Asp, even

dx.doi.org/10.1021/ja410836g | J. Am. Chem. Soc. 2014, 136, 3475−3482

though the exact S−H stretching vibration has not been identified.[22] The present study shows that the S−H group is free from hydrogen bonding. An indirect hydrogen bond between the Asp and Cys has been suggested by the X-ray structure[11] and theoretical calculations,[14,52] the latter proposing that the Cys S−H group donates a hydrogen bond to Thr127 in ChR2. In our view, this is unlikely because the S−H vibration frequency at 2590−2580 cm^{-1} indicates the absence of hydrogen bond (Figure 2). Recent time-resolved FTIR spectroscopy study reported that the Asp in the DC gate is a proton donor to the Schiff base during the photocycle of ChR2.[53] However, from the spectral signature of an H/D unexchangeable Asp in Figure 2, one could argue that Asp in the DC gate may not be a part of the proton pathway, at least in the C1C2 chimera. Similar spectral bands unaffected by H/D exchange were observed for the Asp in the DC gate of ChR2.[50,54]

CONCLUSIONS

For the first time, we report on FTIR signals of protein-bound water molecules in ChR. ChR exhibits an O−D water stretch at 2378 cm^{-1}, which suggests the presence of a strongly hydrogen-bonded water molecule. This implies that ChR has a light-driven proton-pump activity, which is consistent with the recent electrophysiological measurements.[18] It should be however noted that the role of water may be different, because water-containing hydrogen-bonding network in ChR is different from other microbial rhodopsins. Although microbial and animal rhodopsins show changes of 2−6 and 6−8 water bands, respectively, upon retinal isomerization at 77 K, we observed 9 water bands for ChR, suggesting the presence of additional water molecules in the channel cavity. Mutation study revealed a unique hydrogen-bonding network in ChR, where the Schiff base forms a direct hydrogen bond to the counterion (Glu162), while a strongly hydrogen-bonded water molecule bridges Asp292 and Lys132. At present, the functional importance of the unique hydrogen bond of the Schiff base is unclear. Further studies will lead to understanding of the functional role of the hydrogen-bonding network for the light-gated cation channel function.

EXPERIMENTAL SECTION

The C1C2 chimera of ChR was prepared as described previously.[11] Briefly, the C1C2 chimera with tobacco etch virus protease (TEV) cleavage site, the coding sequence of enhanced GFP (EGFP) and the His_8 tag at the C-terminus was expressed in Sf+ insect cells. Membrane fractions from disrupted cells were solubilized with a buffer containing 2.5% (w/v) *n*-dodecyl-*β*-D-maltoside (DDM) and 0.5% (w/v) cholesteryl hemisuccinate, and purified using Ni-NTA resin. EGFP-His_8-tag was cleaved with TEV protease. Then the sample mixture was passed through Ni-NTA resin again to remove the cleaved His-tagged EGFP and TEV protease. The C1C2 sample was further purified by size-exclusion chromatography.

For the FTIR spectroscopy, the C1C2 was reconstituted into phosphatidyl glycerol (PG) liposomes with a protein-to-lipid molar ratio of 1:30 by removing DDM with Bio-Beads (SM-2, Bio-Rad). The reconstituted sample was washed with 2 mM Na/phosphate buffer (pH 7.0), put onto a BaF_2 window and dried with an aspirator. Low-temperature FTIR spectroscopy was applied to the films hydrated with H_2O, D_2O, or $D_2{}^{18}O$ at 77 K, as previously described.[16,17] For the formation of ChR_K, the samples were irradiated with 450 nm light (by use of an interference filter) for 2 min. For the reversion from ChR_K to the original state, the samples were irradiated with >550 nm light for 1 min. For each measurement, 128 interferograms were accumulated, and 96 recordings were averaged.

ASSOCIATED CONTENT

Supporting Information

Absolute absorption spectra of ChR film hydrated with H_2O and D_2O, light-induced difference spectra of ChR film hydrated with D_2O and $D_2{}^{18}O$ in the 4000−850 cm^{-1} and enlarged regions, the difference spectra of mutants, number of water bands in various rhodopsins, and vibrational frequencies of the Schiff base in various rhodopsins. This material is available free of charge via the Internet at http://pubs.acs.org.

AUTHOR INFORMATION

Corresponding Author

kandori@nitech.ac.jp

Notes

The authors declare no competing financial interest.

ACKNOWLEDGMENTS

We thank Drs. Ryuichiro Ishitani and Kota Katayama for valuable discussions and Ms. Arisa Kurabayashi for technical assistance. This work was supported by grants from Japanese Ministry of Education, Culture, Sports, Science and Technology to H.K. (22247024, 25104009) and O.N. (24227004).

REFERENCES

(1) Deisseroth, K. *Nature Methods* **2011**, *8*, 26−29.
(2) Hegemann, P.; Möglich, A. *Nature Methods* **2011**, *8*, 39−42.
(3) Nagel, G.; Ollig, D.; Fuhrmann, M.; Kateriya, S.; Musti, A. M.; Bamberg, E.; Hegemann, P. *Science* **2002**, *296*, 2395−2398.
(4) Sineshchekov, O.; Jung, K.-H.; Spudich, J. L. *Proc. Natl. Acid. Sci. U.S.A.* **2002**, *99*, 8689−8694.
(5) Zhang, F.; Wang, L. P.; Brauner, M.; Liewald, J. F.; Kay, K.; Watzke, N.; Wood, P. G.; Bamberg, E.; Nagel, G.; Gottschalk, A.; Deisseroth, K. *Nature* **2007**, *446*, 633−639.
(6) Chow, B. Y.; Han, X.; Dobry, A. S.; Qian, X.; Chuong, A. S.; Li, M.; Henninger, M. A.; Belfort, G. M.; Lin, Y.; Monahan, P. E.; Boyden, E. S. *Nature* **2010**, *463*, 98−102.
(7) Tye, K. M.; Deisseroth, K. *Nature Rev. Neurosci.* **2012**, *13*, 251−266.
(8) Ernst, O. P.; Lodowski, D. T.; Elstner, M.; Hegemann, P.; Brown, L. S.; Kandori, H. *Chem. Rev.* **2014**, *114*, 126−163.
(9) Lanyi, J. K. *Annu. Rev. Physiol.* **2004**, *66*, 665−688.
(10) Essen, L.-O. *Curr. Opin. Struct. Biol.* **2012**, *12*, 516−522.
(11) Kato, H. E.; Zhang, F.; Yizhar, O.; Ramakrishnan, C.; Nishizawa, T.; Hirata, K.; Ito, J.; Aita, Y.; Tsukazaki, T.; Hayashi, S.; Hegemann, P.; Maturana, A. D.; Ishitani, R.; Deisseroth, K.; Nureki, O. *Nature* **2012**, *482*, 369−374.
(12) Kandori, H. *Biochim. Biophys. Acta* **2000**, *1460*, 177−191.
(13) Freier, E.; Wolf, S.; Gerwert, K. *Proc. Natl. Acad. Sci. U.S.A.* **2011**, *28*, 11435−11439.
(14) Watanabe, C. H.; Welke, K.; Sindhikara, J. D.; Hegemann, P.; Elstner, M. *J. Mol. Biol.* **2013**, *425*, 1795−1814.
(15) Kandori, H. *Biochim. Biophys. Acta* **2004**, *1658*, 72−79.
(16) Kandori, H. In *Supramolecular Photochemistry: Controlling Photochemical Processes*; Ramamurthy, V., Inoue, Y., Eds.; John Wiley & Sons, Inc.: Hoboken, NJ, 2011, pp 571−596.
(17) Muroda, K.; Nakashima, K.; Shibata, M.; Demura, M.; Kandori, H. *Biochemistry* **2012**, *51*, 4677−4684.
(18) Feldbauer, K.; Zimmermann, D.; Pintschovius, V.; Spitz, J.; Bamann, C.; Bamberg, E. *Proc. Natl. Acad. Sci. U.S.A.* **2009**, *106*, 12317−12322.
(19) Nack, M.; Radu, I.; Schuttz, B. J.; Resler, T.; Bondar, A. N.; del Val, C.; Abbruzzetti, S.; Viappiani, C.; Bamann, C.; Bamberg, E.; Heberle, J. *FEBS Lett.* **2012**, *586*, 1344−1348.
(20) Ritter, E.; Stehfest, K.; Berndt, A.; Hegemann, P.; Bartl, F. J. *J. Biol. Chem.* **2008**, *283*, 35033−35041.

(21) Radu, I.; Bamann, C.; Nack, M.; Nagel, G.; Bamberg, E.; Heberle, J. *J. Am. Chem. Soc.* **2009**, *131*, 7313−7319.
(22) Nack, M.; Radu, I.; Gossing, M.; Bamann, C.; Bamberg, E.; von Mollard, G. F.; Heberle, J. *Photochem. Photobiol. Sci.* **2010**, *9*, 194−198.
(23) Nack, M.; Radu, I.; Bamann, C.; Bamberg, E.; Heberle, J. *FEBS Lett.* **2009**, *583*, 3676−3680.
(24) Baasov, T.; Friedman, N.; Sheves, M. *Biochemistry* **1987**, *26*, 3210−3217.
(25) Eisenhauer, K.; Kuhne, J.; Ritter, E.; Berndt, A.; Wolf, S.; Bartl, F.; Hergmann, P.; Gerwert, K. *J. Biol. Chem.* **2012**, *287*, 6904−6911.
(26) Li, H.; Thomas, G. J., Jr. *J. Am. Chem. Soc.* **1991**, *113*, 456−462.
(27) Kandori, H.; Kinoshita, N.; Shichida, Y.; Maeda, A.; Needleman, R.; Lanyi, J. K. *J. Am. Chem. Soc.* **1998**, *120*, 5828−5229.
(28) Shibata, M.; Kandori, H. *Biochemistry* **2005**, *44*, 7406−7413.
(29) Ikeda, D.; Furutani, Y.; Kandori, H. *Biochemistry* **2007**, *46*, 5365−5373.
(30) Hashimoto, K.; Choi, A. R.; Furutani, Y.; Jung, K.-H.; Kandori, H. *Biochemistry* **2010**, *49*, 3343−3350.
(31) Sumii, M.; Furutani, Y.; Waschuk, S. A.; Brown, L. S.; Kandori, H. *Biochemistry* **2005**, *44*, 15159−15166.
(32) Kandori, H.; Furutani, Y.; Shimono, K.; Shichida, Y.; Kamo, N. *Biochemistry* **2001**, *40*, 15693−15698.
(33) Shibata, M.; Muneda, N.; Sasaki, T.; Shimono, K.; Kamo, N.; Demura, M.; Kandori, H. *Biochemistry* **2005**, *44*, 12279−12286.
(34) Furutani, Y.; Kawanabe, A.; Jung, K.-H.; Kandori, H. *Biochemistry* **2005**, *44*, 12287−12296.
(35) Furutani, Y.; Bezerra, A. G., Jr.; Waschuk, S.; Sumii, M.; Brown, L. S.; Kandori, H. *Biochemistry* **2004**, *43*, 9636−9646.
(36) Furutani, Y.; Shichida, Y.; Kandori, H. *Biochemistry* **2003**, *42*, 9619−9625.
(37) Ota, T.; Furutani, Y.; Terakita, A.; Shichida, Y.; Kandori, H. *Biochemistry* **2006**, *45*, 2845−2851.
(38) Katayama, K.; Furutami, Y.; Imai, H.; Kandori, H. *Biochemistry* **2012**, *51*, 1126−1133.
(39) Kandori, H.; Belenky, M.; Herzfeld, J. *Biochemistry* **2002**, *41*, 6026−6031.
(40) Tanimoto, T.; Shibata, M.; Belenky, M.; Herzfeld, J.; Kandori, H. *Biochemistry* **2004**, *43*, 9439−9447.
(41) Luecke, H.; Schobert, B.; Richter, H.-T.; Cartailler, J.-P.; Lanyi, J. K. *J. Mol. Biol.* **1999**, *291*, 899−911.
(42) Moltke, S.; Krebs, M. P.; Mollaaghababa, R.; Khorana, H. G.; Heyn, M. *Biophys. J.* **1995**, *69*, 2074−2083.
(43) Yizhar, O.; Fenno, L. E.; Davidson, T. j.; Mogri, M.; Deisseroth, K. *Neuron* **2011**, *71*, 9−34.
(44) Okada, T.; Fujiyoshi, Y.; Silow, M.; Navarro, J.; Landau, E. M.; Shichida, Y. *Proc. Natl. Acad. Sci. U.S.A.* **2002**, *99*, 5982−5987.
(45) Vogeley, L.; Sineshchekov, O. A.; Trivedi, V. D.; Sasaki, J.; Spudich, J. L.; Luecke, H. *Science* **2004**, *306*, 1390−1393.
(46) Luecke, H.; Schobert, B.; Stagno, J.; Imasheva, E. S.; Wang, J. H.; Balashov, S. P.; Lanyi, J. K. *Proc. Natl. Acad. Sci. U.S.A.* **2008**, *105*, 16561−16565.
(47) Gushchin, I.; Chervakov, P.; Kuzmichev, P.; Popv, A. N.; Round, E.; Borshchevskiy, V.; Ishchenko, A.; Petrovskaya, L.; Chupin, V.; Dolgikh, D. A.; Arseniev, A. A.; Kirpichnikov, M.; Gordeliy, V. *Proc. Natl. Acad. Sci. U.S.A.* **2013**, *110*, 12631−12636.
(48) Imasheva, E. S.; Balashov, S. P.; Wang, J. M.; Lanyi, J. K. *Photochem. Photobiol.* **2006**, *82*, 1406−1413.
(49) Miranda, M. R. M.; Choi, A. R.; Shi, L.; Bezerra, A. G., Jr.; Jung, K.-H.; Brown, L. S. *Biophys. J.* **2009**, *96*, 1471−1481.
(50) Neumann-Verhoefen, M.-K.; Neumann, K.; Bamann, C.; Radu, I.; Heberle, J.; Bamberg, E.; Wachtveitl, J. *J. Am. Chem. Soc.* **2013**, *135*, 6968−6976.
(51) Berndt, A.; Yizhar, O.; Gunaydin, L. A.; Hegemann, P.; Deisseroth, K. *Nature Neurosci.* **2009**, *12*, 229−234.
(52) Welke, K.; Watanabe, H. C.; Wolter, T.; Gaus, M.; Elstner, M. *Phys. Chem. Chem. Phys.* **2013**, *15*, 6651−6659.
(53) Lórenz-Fonfría, V. A.; Resler, T.; Krause, N.; Nack, M.; Gossing, M.; von Mollard, G. F.; Bamann, C.; Bamberg, E.; Schlesinger, R.; Heberle, J. *Proc. Natl. Acad. Sci. U.S.A.* **2013**, *106*, E1273−E1281.
(54) Ernst, O. P.; Sánchez Murcia, P. A.; Daldrop, P.; Tsunoda, S.; Kateriya, S.; Hegemann, P. *J. Biol. Chem.* **2008**, *283*, 1637−1643.
(55) Kandori, H.; Kinoshita, N.; Shichida, Y.; Maeda, A. *J. Phys. Chem. B* **1998**, *102*, 7899−7905.
(56) Tanimoto, T.; Furutani, Y.; Kandori, H. *Biochemistry* **2003**, *42*, 2300−2306.
(57) Shimono, K.; Furutani, Y.; Kamo, N.; Kandori, H. *Biochemistry* **2003**, *42*, 7801−7806.